The Astrophysical Journal, 627:L133–L136, 2005 July 10

A FIRST LOOK WITH *CHANDRA* AT SGR 1806−20 AFTER THE GIANT FLARE: SIGNIFICANT SPECTRAL SOFTENING AND RAPID FLUX DECAY

N. Rea,[1,2,3] A. Tiengo,[4,5] S. Mereghetti,[4] G. L. Israel,[2] S. Zane,[6] R. Turolla,[7] and L. Stella[2]
Received 2005 March 18; accepted 2005 May 17; published 2005 June 17

ABSTRACT

We report on the results of an ∼30 ks *Chandra* pointing of the soft gamma-ray repeater SGR 1806−20, the first X-ray observation with high spectral resolution performed after the 2004 December 27 giant flare. The source was found in a bursting active phase and with a significantly softer spectrum than that of the latest observations before the giant flare. The observed flux in the 2–10 keV range was $\sim 2.2 \times 10^{-11}$ ergs cm^{-2} s^{-1}, about 20% lower than that measured 3 months before the event. This indicates that although its giant flare was ≈100 times more intense than those previously observed in two other soft gamma-ray repeaters, the postflare X-ray flux decay of SGR 1806−20 has been much faster. The pulsed fraction was ∼3%, a smaller value than that observed before the flare. We discuss the different properties of the postflare evolution of SGR 1806−20 in comparison to those of SGR 1900+14 and interpret the results as strong evidence that a magnetospheric untwisting occurred (or is occurring) after the giant flare.

Subject headings: magnetic fields — pulsars: general — pulsars: individual (SGR 1806−20) — X-rays: stars

1. INTRODUCTION

Soft gamma-ray repeaters (SGRs) are neutron stars that emit short (≲1 s) and energetic ($\lesssim 10^{42}$ ergs s^{-1}) bursts of soft γ-rays. The burst repetition time can vary from seconds to years (Göğüş et al. 2001). During the quiescent state (i.e., outside burst events), these sources are detected as persistent X-ray emitters at a luminosity of $\sim 10^{35}$–10^{36} ergs s^{-1}. Occasionally, SGRs emit much more energetic "giant flares" ($\sim 10^{44}$–10^{45} ergs s^{-1}); these are rare events until recently only reported on two occasions from SGR 0526−66 and SGR 1900+14 (Mazets et al. 1979; Hurley et al. 1999).

Several characteristics of SGRs, including their bursting activity, are explained in the context of the "magnetar" model (Duncan & Thompson 1992; Thompson & Duncan 1995). Magnetars are neutron stars, the emission of which is powered by the decay of an ultrastrong magnetic field ($\sim 10^{14}$–10^{15} G). In this model the frequent short bursts are associated with small cracks in the neutron star crust, while the giant flares are linked to global rearrangements of the star magnetosphere.

On 2004 December 27, SGR 1806−20 emitted an exceptionally powerful giant flare, with an initial hard spike lasting 0.2 s, followed by an ∼600 s long pulsating tail (Borkowski et al. 2004; Hurley et al. 2004; Mazets et al. 2004). The prompt emission saturated almost all γ-ray detectors, except for those on the *Geotail* spacecraft, which provided a reliable measurement of the peak intensity (Terasawa et al. 2005). The isotropic luminosity above 50 keV was $\sim 6.47 \times 10^{47}$ ergs s^{-1} (for a distance of 15 kpc), hundreds of times higher than that of the two giant flares previously observed from other SGRs. Following this event, afterglow emission similar to that commonly observed in γ-ray bursts has been observed in the radio band, with a resolved extended structure (Cameron et al. 2005; Gaensler et al. 2005) and possibly also at hard X-ray energies (Mereghetti et al. 2005a). The extremely accurate localization (∼0″.1) obtained with the radio data made possible the identification of a variable infrared counterpart (Kosugi et al. 2005; Israel et al. 2005).

Here we report the results of a *Chandra* Director's Discretionary Time observation of SGR 1806−20, which provided the first X-ray data set with high spectral resolution after the giant flare.

2. OBSERVATION

Chandra observed SGR 1806−20 for ∼30 ks with the Advanced CCD Imaging Spectrometer (ACIS) instrument on 2005 February 8. In order to avoid pileup and perform pulse-phase–resolved spectroscopy, the source was observed in the continuous clocking (CC) mode, which provides a time resolution of 2.85 ms and imaging along a single direction. The source was positioned in the back-illuminated ACIS-S3 CCD at the nominal target position. Standard processing of the data was performed by the *Chandra* X-ray Center to level 1 and level 2 (processing software DS ver. 7.5.0.1). The data were reprocessed using the CIAO software (ver. 3.2) and the *Chandra* calibration files (CALDB ver. 3.0.0).

Since in the CC mode the events are tagged with the times of the frame store, we corrected the times for the variable delay due to the spacecraft dithering and telescope flexure, starting from level 1 data and assuming that all photons were originally detected at the target position.[8] We filtered the data to exclude events with *ASCA* grades 1, 5, and 7, hot pixels, bad columns, and possible afterglow events (residual charge from the interaction of a cosmic ray in the CCD). In the data processing and analysis, we always used the specific bad-pixel file of this observation rather than those provided with the standard calibration files. After such filtering, the observing time was 29.1 ks.

[1] SRON–National Institute for Space Research, Sorbonnelan 2, 3584 CA, Utrecht, Netherlands.

[2] INAF–Astronomical Observatory of Rome, Via Frascati 33, 00040, Monteporzio Catone (Rome), Italy.

[3] Marie Curie Fellow to NOVA, The Netherlands Research School in Astronomy.

[4] Istituto di Astrofisica Spaziale e Fisica Cosmica "G. Occhialini," Via Bassini 15, 20133, Milan, Italy.

[5] Università degli Studi di Milano, Dipartimento di Fisica, Via Celoria 16, I-20133 Milan, Italy.

[6] Mullard Space Science Laboratory, University College of London, Holmbury St. Mary, Dorking Surrey, RH5 6NT, UK.

[7] University of Padua, Department of Physics, Via Marzolo 8, 35131, Padua, Italy.

[8] See the *Chandra* Science Threads at http://asc.harvard.edu/ciao/threads/index.html for details.

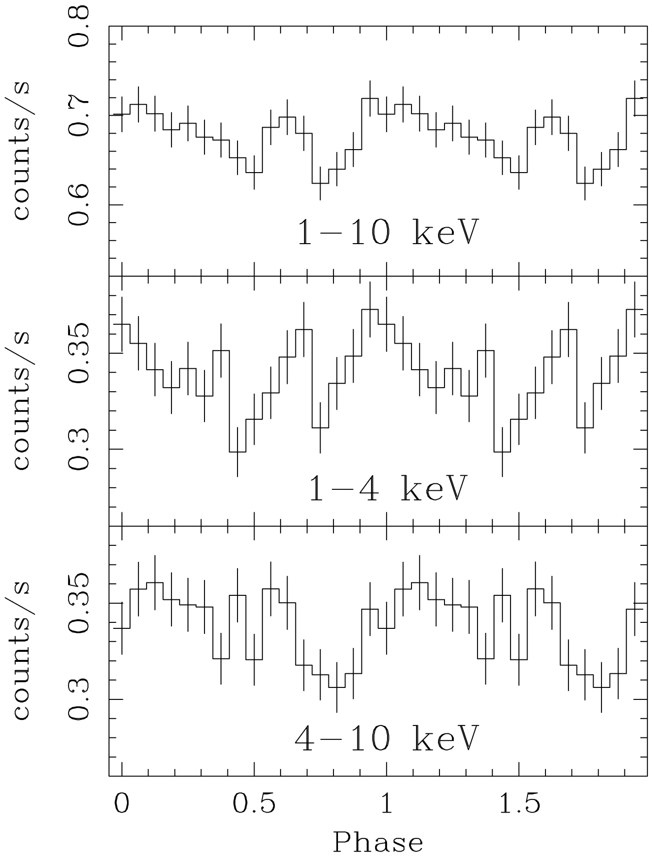

FIG. 1.—Folded pulse profiles in the total (1–10 keV; *top*), soft (1–4 keV; *middle*) and hard (4–10 keV; *bottom*) energy ranges.

3. RESULTS

3.1. *Timing*

In order to carry out a timing analysis, we extracted the events in the 1–10 keV energy range from a region of 5 × 5 pixels around the source position and corrected their arrival times to the barycenter of the solar system. We looked for the presence of bursts by binning the counts in intervals of 0.2 s and searching for excesses above a count threshold corresponding to a chance occurrence of 0.1% (taking into account the total number of bins). In this way we identified a single burst lasting about 0.5 s at 00:38:25 UT on February 9.

The relatively poor statistics and small pulsed fraction did not permit us to determine the pulse period independently from the *Chandra* data. We therefore adopted a period of $P = 7.560023$ s, measured during an almost simultaneous *R*XTE observation (P. Woods 2005, private communication). For this period the Z_m^2 test (Buccheri et al. 1983) gave a significance of 3.5 σ for a number of harmonics $m = 3$ (or 2.9 σ for $m = 2$). The resulting pulse profiles folded in 16 phase bins are shown in Figure 1 for three different energy ranges (1–10, 1–4, and 4–10 keV). The modulation is rather low, with some evidence of a double-peaked profile and possibly an energy-dependent shape. By using two sine functions to fit the pulse profile in the total energy range, we obtain pulsed fraction values of $PF_1 = 3.0\% \pm 1.6\%$ and $PF_2 = 2.6\% \pm 1.6\%$[9] for the fundamental and the second harmonic, respectively.

3.2. *Spectroscopy*

The source spectrum was extracted from a rectangular region of 5 × 25 pixels around the source position, and the background was taken independently from a source-free region in the same chip.

Since the CC mode has not yet been calibrated, standard threads for spectral analysis are not available, and the timed-exposure mode response matrix files (RMFs) and ancillary response files (ARFs) are generally used. In order to extract the RMF, we first created a weighted image, rebinning by a factor of 8. We then used it in the `mkacisrmf` tool, with an energy grid ranging from 0.3 to 10 keV in 5 eV increments. Using this RMF and the aspect histogram created with the aspect solution for this observation (`asphist`), we generated the appropriate ARF file for the source position. Considering that only a few counts were detected below 2 keV, due to the high interstellar absorption and to uncertainties in the instrument calibrations at these low energies, we restricted our fits to the 2–8 keV energy range. All the fits were performed using XSPEC (ver. 11.3).

Equally good results were obtained using either a power law (photon index $\Gamma \sim 1.8$) or a thermal bremsstrahlung model ($kT_{\rm brem} \sim 10$ keV), whereas single blackbody and neutron star atmosphere models gave unacceptable fits ($\chi^2_\nu \sim 2.1$ in both cases). The results of the acceptable fits are summarized in Table 1, where we report for comparison also those fits obtained in 2004 September, before the giant flare, with *XMM-Newton* (Mereghetti et al. 2005b). The best-fit power-law spectrum is shown in Figure 2. The absorption derived from the *Chandra* data was consistent with the preflare value. Keeping the absorption fixed at the *XMM-Newton* value yielded a photon index

[9] We define PF as the semiamplitude of the two sine functions; all errors in the text are at the 90% confidence level.

TABLE 1
SPECTRAL RESULTS FOR SGR 1806−20

Model	N_H (10^{-22} cm^{-2})		kT (keV)	R_{bb}[a] (km)	Flux[b] (ergs s^{-1}cm^{-2})	χ^2_{red} (dof)
XMM-Newton Preflare (Mereghetti et al. 2005b; Obs. C)						
Power-law	6.69 ± 0.13	1.51 ± 0.03	…	…	2.65	1.37 (72)
Power-law+blackbody	$6.51^{+0.37}_{-0.27}$	$1.21^{+0.14}_{-0.12}$	$0.79^{+0.09}_{-0.12}$	$1.9^{+0.7}_{-0.3}$	2.65	0.93 (70)
Chandra Postflare (This Work)						
Power-law	7.1 ± 0.4	1.8 ± 0.1	…	…	2.2	0.91 (47)
Power-law	6.69 fixed	1.77 ± 0.05	…	…	2.2	0.91 (48)
Thermal bremsstrahlung	6.4 ± 0.4	…	$10.7^{+3.6}_{-2.3}$	…	2.2	0.90 (47)
Power-law+blackbody	$7.5^{+2.3}_{-2.1}$	$1.78^{+0.29}_{-1.15}$	<0.93	<47.1	2.2	0.93 (45)
Power-law+blackbody	6.51 fixed	1.46 ± 0.06	0.79 fixed	1.9 fixed	2.2	0.93 (48)

[a] For a distance of 15 kpc; errors in the table are given at the 90% confidence level.
[b] In the 2–10 keV energy band and in units of 10^{-11}; not corrected for the absorption.

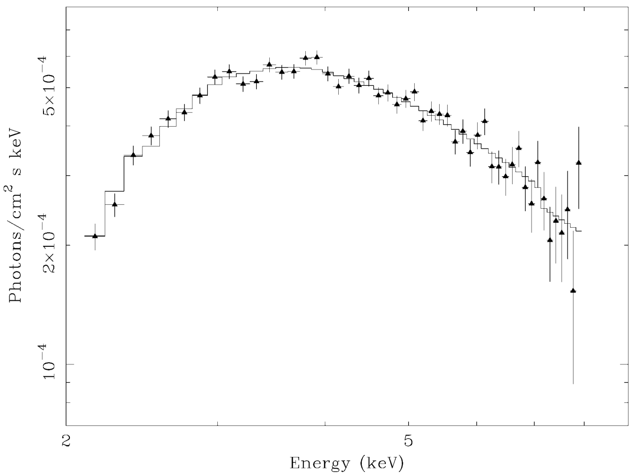

FIG. 2.—Postflare *Chandra* SGR 1806−20 spectrum fitted with an absorbed power law.

$\Gamma = 1.77 \pm 0.05$ and a flux of $(2.2 \pm 0.2) \times 10^{-11}$ ergs cm^{-2} s^{-1} (2–10 keV; not corrected for absorption).

The addition of a blackbody component to the absorbed power law was not required, contrary to the case of the *XMM-Newton* spectrum of 2004 September, which had a higher statistics. Even by performing the fit of the *Chandra* data in the wider 0.3–10 keV range, the inclusion of an additional blackbody component does not improve significantly the fit (*F*-test probability = 0.012). Note, however, that the presence of a blackbody with the temperature and normalization as seen with *XMM-Newton* is compatible with the *Chandra* data (see Table 1).

We performed pulse-phase–resolved spectroscopy by extracting the spectra for three phase intervals, corresponding to the rise and the decay of the broad peak and to the narrow peak (see Fig. 1). The resulting spectral parameters were, to within the uncertainties, compatible with those of the phase-averaged spectrum. This is not surprising, considering that the pulsed component represents only ~3% of the total emission.

We do not find any evidence for absorption or emission features in the source-averaged and phase-resolved spectra. We derived upper limits as a function of the line energy and width (σ_E) by adding Gaussian lines to the continuum model. For the phase-averaged spectrum, the 3 σ upper limit on the equivalent width of narrow lines is ~80 eV. The corresponding values for broad lines are 110 and 135 eV (for $\sigma_E = 0.1$ and 0.2 keV, respectively).

The burst identified in the *Chandra* data does not contain enough counts for a meaningful spectral analysis.

3.3. *Extended Emission and Structures*

In order to search for extended X-ray emission or structures around the source, we studied the radial profiles of SGR 1806−20. Since the CC mode has only one-dimensional imaging capability, we first generated an image of the one-dimensional strip in the 0.3–8 keV band and then subtracted an average count rate aimed to remove instrumental and cosmic X-ray background (Markevitch & Vikhlinin 2001). We then produced a one-dimensional surface-brightness distribution using the same method as for a two-dimensional radial profile. Since calibration point-spread functions are not available for the CC mode, we similarly extracted the radial profile from a CC-mode observation (ObsID 4523) of RX J0806+1527. This latter source is known to be pointlike and has both an X-ray flux and spectrum rather similar to those of our target (Israel et al. 2003).

The ratio between the radial profiles of the two sources did not show any evidence of a significant extended emission or structures within 30″ around our target, with a 3 σ upper limit in flux of $<10^{-14}$ ergs s^{-1} cm^{-2} (in the 4″–30″ range of radii).

4. DISCUSSION

This *Chandra* X-ray observation of SGR 1806−20 is the first with an imaging instrument after the 2004 December giant flare. It is therefore interesting to compare the results with the preflare properties of the source, as measured with *XMM-Newton* in 2004 September–October (Mereghetti et al. 2005b).

The *Chandra* data clearly indicate that the spectrum softened significantly; we obtained a power law with $\Gamma \sim 1.8$. This must be compared with the preflare values $\Gamma \sim 1.2$ (with the inclusion of the blackbody) or $\Gamma \sim 1.5$–1.6 (in the single power-law model; see Table 1). The flux measured with *Chandra* is ~20% lower than the preflare value, but still significantly higher than the historical flux level of $\sim1.3 \times 10^{-11}$ ergs cm^{-2} s^{-1} observed before the second half of 2004.[10] Another difference with respect to the preflare properties is the smaller pulsed fraction (which changed from about 10% to 3%). The pulse profile is also now double-peaked.

The postflare evolution of SGR 1806−20 shows both similarities and differences when compared to that of SGR 1900+14, the only other case in which good spectral X-ray data have been collected after a giant flare. In particular, a significant spectral softening was observed to accompany the postgiant flare evolution of SGR 1900+14 also (Woods et al. 1999, 2001). Even though the SGR 1806−20 giant flare was 2 orders of magnitude more energetic than that of SGR 1900+14 (and of SGR 0526–66 as well), it was followed by a very rapid decay of the X-ray luminosity. We find that the source flux has dropped below the preflare level after about 1 month, much faster than what was observed after the SGR 1900+14 giant flare. This suggests that the postflare softening, a feature common to both sources, is unrelated to the flare energetics and the decay rate of the X-ray flux after the flare.

SGR 1806−20 and SGR 1900+14 also exhibit quite a different behavior in the evolution of their timing properties. The pulse profile of SGR 1900+14 changed from a complex, multipeaked pattern to a simpler sinusoidal shape. The preflare pulse shape has not yet been recovered, a possible signature of a permanent rearrangement of the star magnetosphere (Woods et al. 2001). In the case of SGR 1806−20, the pulse profile changed from being almost sinusoidal to double-peaked. The data obtained during the giant flare indicate a multipeak structure, with a time-variable and energy-dependent contribution of the different peaks (Palmer et al. 2005; Hurley et al. 2005; Mereghetti et al. 2005a). This may indicate a different evolution of the geometry of the magnetosphere. Moreover, while the pulsed fraction in SGR 1900+14 did not change significantly after the flare, we found that in SGR 1806−20 it decreased by about a factor of 3.

XMM-Newton observations of SGR 1806−20 carried out few months before the giant flare have shown an increase of both the spectral hardening and the spin-down rate with respect to historical values (Mereghetti et al. 2005b). In the picture proposed by Thompson et al. (2002), a twisted internal mag-

[10] Note that before the giant flare, the flux was increasing and the flux level was larger than its historical average (see Mereghetti et al. 2005b).

netic field stresses the star's solid crust, producing a progressive increase in the twist angle of the external field lines. A giant flare is produced when the crust is no longer able to respond (quasi)plastically to the imparted stresses and finally cracks. The crustal fracturing is accompanied by a simplification of the external magnetic field, with a (partial) untwisting of the magnetosphere. The spectral softening after the 2004 December 27 event appears consistent with such a picture. In fact, the situation after the flare is somehow opposite to what occurred before the flare, when the twist was increasing. The sudden drop of the external twist that followed the giant flare resulted in a decrease of the optical depth to resonant cyclotron scattering in the magnetosphere and hence in a steepening of the power-law spectrum.

The main observational consequences of a magnetospheric untwisting, namely a decrease in the X-ray flux, a softening of the spectrum, and a decrease of the pulsed fraction (Thompson et al. 2002; Hurley et al. 2005), appear to be present in this first postflare observation.

We thank Harvey Tananbaum for granting Director's Discretionary Time for this observation, and the whole *Chandra* team for the precious help and the patience. We also thank P. Woods and his working group for the information on the *RXTE* results. N. R. thanks M. Méndez and L. Kuiper for their advice, and the SRON HEA division for its hospitality. N. R. is supported by a Marie Curie Training Grant (HPMT-CT-2001-00245) for Ph.D. students to NOVA, The Netherlands Research School in Astronomy. This work was partially supported through MIUR and ASI grants.

REFERENCES

Borkowski, J., Gotz, D., Mereghetti, S., Mowlavi, N., Shaw, S., & Turler, M. 2004, GCN Circ. 2920, http://gcn/gsfc.nasa.gov/gcn/gcn3/2920.gcn3
Buccheri, R., et al. 1983, A&A, 128, 245
Cameron, P. B., et al. 2005, Nature, submitted (astro-ph/0502428)
Duncan, R. C., & Thompson, C. 1992, ApJ, 392, L9
Gaensler, B. M., et al. 2005, Nature, 434, 1104
Göğüş, E., et al. 2001, ApJ, 558, 228
Hurley, K., et al. 1999, Nature, 397, 41
———. 2004, GCN Circ. 2921, http://gcn/gsfc.nasa.gov/gcn/gcn3/2921.gcn3
———. 2005, Nature, 434, 1098
Israel, G. L., et al. 2003, ApJ, 598, 492
———. 2005, A&A, in press (astro-ph/0506095)
Kosugi, G., Ogasawara, R., & Terada, H. 2005, ApJ, 623, L125
Markevitch, M., & Vikhlinin, A. 2001, ApJ, 563, 95
Mazets, E. P., Golenetskii, S., Aptekar, R., Frederiks, D., Pal'Shin, V., & Cline, T. 2004, GCN Circ. 2922, http://gcn/gsfc.nasa.gov/gcn/gcn3/2922.gcn3
Mazets, E. P., et al. 1979, Nature, 282, 587
Mereghetti, S., Götz, D., von Kienlin, A., Rau, A., Lichti, G., Weidenspointner, G., & Jean, P. 2005a, ApJ, 624, L105
Mereghetti, S., et al. 2005b, ApJ, 628, in press (astro-ph/0502417)
Palmer, D. M., et al. 2005, Nature, 434, 1107
Terasawa, T., et al. 2005, Nature, 434, 1110
Thompson, C., & Duncan, R. C. 1995, MNRAS, 275, 255
Thompson, C., Lyutikov, M., & Kulkarni, S. 2002, ApJ, 574, 355
Woods, P., Kouveliotou, C., Gögüs, E., Finger, M. H. Swank, J., Smith, D. A., Hurley, K., & Thompson, C. 2001, ApJ, 522, 748
Woods, P., et al. 1999, ApJ, 518, L103